

Benchmark Computations of Nearly Degenerate Singlet and Triplet states of N-heterocyclic Chromophores : I.

Wavefunction-based Methods

Shamik Chanda and Sangita Sen*

Department of Chemical Sciences

Indian Institute of Science Education and Research (IISER) Kolkata

Nadia, Mohanpur-741246, WB, India

Abstract

In this paper we investigate the role of electron correlation in predicting the S_1-S_0 and T_1-S_0 excitation energies and hence, the singlet-triplet gap (ΔE_{ST}) in a set of cyclazines which act as templates for potential candidates for 5th generation Organic Light Emitting Diode (OLED) materials. This issue has recently garnered much interest with the focus being on the inversion of the ΔE_{ST} , although experiments have indicated near degenerate levels with both positive and negative being within the experimental error bar (*J. Am. Chem. Soc.* 1980, 102: 6068 , *J. Am. Chem. Soc.* 1986, 108: 17). We have carried out a systematic and exhaustive study of various excited state electronic structure methodologies and identified the strengths and shortcomings of the various approaches and approximations in view of this challenging case. We have found that near degeneracy can be achieved either with a proper balance of static and dynamic correlation in multireference theories or with state-specific orbital corrections including its coupling with correlation. The role of spin contamination is also discussed. Eventually, this paper seeks to produce benchmark numbers for establishing cheaper theories which can then be used for screening derivatives of these templates with desirable optical and structural properties. Additionally we would like to point out that the use of DLPNO-STEOM-CCSD as the benchmark for ΔE_{ST} (as used in *J. Phys. Chem. A* 2022, 126: 8: 1378, *Chem. Phys. Lett.* 2021, 779: 138827) is not a suitable benchmark for this class of molecules.

Keywords: Inverted Singlet-triplet, electron correlation, OLED molecules, cyclazine, azine, excitation energy, TADF.

*Email: sangita.sen@iiserkol.ac.in

I. INTRODUCTION

A new generation of materials have been proposed for making Organic Light Emitting Diodes (OLEDs) which can potentially have 100% quantum yield[1, 2]. The design principle involves having near-degenerate S_1 and T_1 states such that the electrons that have undergone intersystem-crossing (ISC) from S_1 to T_1 can be brought back to S_1 by reverse intersystem crossing (RISC) through thermal activation and subsequent deexcitation occurs from the S_1 to S_0 state, which leads to thermally activated delayed fluorescence (TADF)[3–5]. It is reasonable to suppose that RISC would be most efficient if no thermal activation was required. This can be achieved if the S_1 - T_1 gap is inverted[6–9]. However, one must not forget that the mechanism of RISC involves vibronic coupling which diminishes with increasing energy gap[10]. Thus, theoretical screening of OLED candidate molecules for large inverted gaps may be counterproductive. In fact, the experimental values for the few candidate molecules which could be synthesized show small positive/negative values[11]. Benchmarking cheaper, mostly density functional approaches, against theories indicating large inverted gaps can thus be misleading. Only static correlation, on the other hand, is very sensitive to the choice of the active space and thus tedious for large scale screening. Supplementing CASSCF with dynamic correlation can often reduce this sensitivity. In this paper we examine the correlation effects captured by various wavefunction-based electronic structure theories and try to arrive at the most accurate correlation model to serve as a benchmark for DFT-based methods. A few preliminary DFT-based computations are presented here while a more detailed study follows in a forthcoming publication[12].

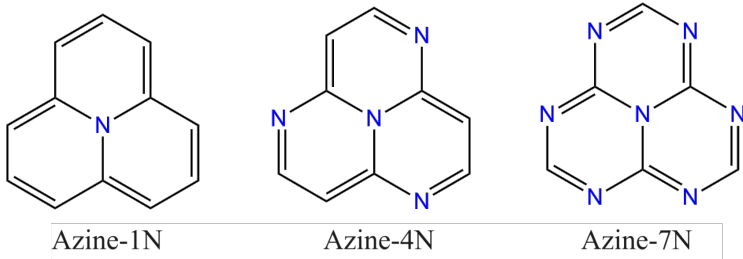


FIG. 1: The molecular templates studied in this paper for inverted singlet-triplet gaps.

Exchange interactions, which stabilise the T_1 state result in T_1 to be typically below the S_1 state with $\Delta E_{ST} > 0$ (Hund’s Law[13]). However, some N-substituted fused ring molecules, such as cyclazines and their derivatives (see Fig. 1) exhibit close to degenerate or inverted

S_1 - T_1 gaps in experiments[1, 2, 11]. Common linear response excited state methods such as Configuration Interaction Singles (CIS)[14, 15], Random Phase Approximation (RPA)[16, 17] or Time-Dependent Density Functional Theory (TD-DFT)[18] which are formulated for treating primarily singly excited states[19] almost always give this gap as positive. While CIS and RPA are theoretically guaranteed to give $\Delta E_{ST} > 0$, TD-DFT can give an inverted gap if the exchange-correlation functional captures sufficient electron correlation which is usually not the case for commonly used functionals. In recent publications[20–22], presence of low-lying excited states with doubly excited character have been indicated to be the crucial criteria for ST inversion[20]. Simply put, greater electron correlations in S_1 relative to T_1 reduce the ST gap leading to a nearly degenerate or even inverted ΔE_{ST} as shown in Fig. 2.

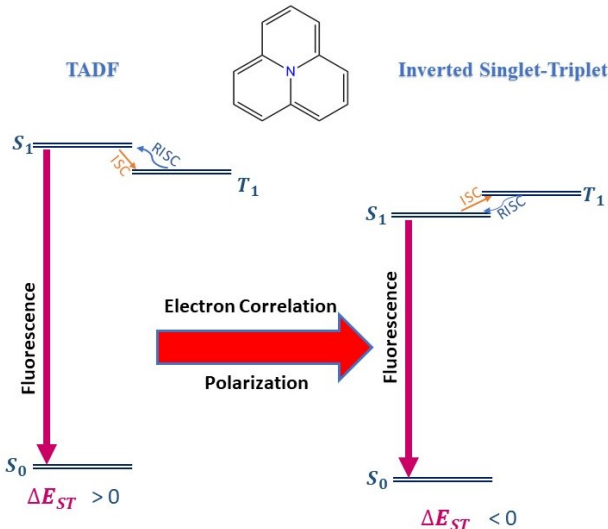


FIG. 2: Violation of Hund's Law

Recently, in this context, azine-1N, azine-4N, azine-7N (heptazine) (see Fig. 1) and related molecules and derivatives have received much interest from the electronic structure community[11, 20–31]. The inability of linear-response time-dependent density functional theory (LR-TDDFT)[18, 32] and the success of wave function techniques such as doubles-corrected configuration interaction singles [CIS(D)][33], and equation of motion coupled cluster singles and doubles (EOM-CCSD)[34, 35] in computing inverted singlet-triplet gaps have been pointed out[20, 21, 36]. A combined DFT/Multireference Configuration Interaction (DFT/MRCI) method to investigate the impact of the negative singlet-triplet gap and the

vibronic coupling in heptazine derivatives was also recently reported[10]. Novel techniques such as spin-component scaled second-order coupled cluster (SCS-CC2)[37], ADC[38], and multireference techniques such as complete active space self-consistent field (CASSCF)[39] and N-electron valence second-order perturbation theory (NEVPT2)[40] have also predicted the inverted singlet-triplet gaps[22, 27]. Recently Loos. et. al.[31] reported benchmark excitation energies for a set of azine and heptazine based molecules using a high level CC3[41] framework. Computationally cheaper domain-based local pair natural orbital (DLPNO) similarity transformed EOM-CCSD (STEOM-CCSD)[42] also inverted the gaps but unfortunately they are far more inverted than predicted by experiments([1, 2]) and inconsistent across various molecules[21, 43].

Among the density functional approaches, the doubles-corrected TDDFT [TDDFT(D)][44] approach with B2PLYP double-hybrid functionals, could achieve inversion[24] but since the DLPNO-STEOM-CCSD was considered as the benchmark, they were dismissed as having inadequate correlation. In this (see Fig. 4), and a forthcoming publication[12] we demonstrate that these functionals are indeed reasonable and it is the DLPNO-STEOM-CCSD which over-inverts. This is an important finding as the TD-DFT framework is very popular for screening molecules for stable molecular structures, peak wavelengths, intensities, colour purity and other desirable structural and optical features. A proper choice or design of a DFT framework is predicated by the availability of a benchmark theory. CC2 and ADC(2) are also possible alternatives with a similar computational cost[22, 31]. In this particular case, the canonical EOM-CCSD may be used but we cannot take advantage of the cost-saving afforded by the similarity transformed EOM (STEOM) approach (see Table I). The aim of our paper is, thus, to suggest the most reliable benchmark theory for this class of molecules and in doing so, to properly establish the necessary physics that needs to be captured to be able to describe the energetics of the optical processes involved here.

A brief comparison of single and multi-reference theories used in this article is given in Sec. II. The computational and technical details is given in Sec III. In Sec IV A, a detailed analysis of the results obtained from single-reference theories are given including CIS, CIS(D), TDHF/RPA, RPA(D)[45], ADC(2) and EOM-CCSD. Then, in Sec IV B, the detailed analysis of the CASSCF for several choices of active electrons and orbitals is carried out for a prototypical molecule, ie. azine-1N. This section also includes the CASSCF, strongly

contracted(SC)-NEVPT2, CASPT2, and FICMRCI results for all the molecules. Finally we summarize our conclusions and discuss the future outlook of this study in Sec V.

II. THEORETICAL DETAILS

Any N-electron wavefunction can be completely described in a given M-orbital basis as a linear combination of all possible Nth order determinants that can be constructed from the M orbitals[46]. However, for the ease of approximation a distinction is made between two subsets of determinants. In a typical electronic state, it is found that a few determinants constructed usually from degenerate or quasi degenerate orbitals have significantly higher coefficients. These determinants are said to constitute static/non-dynamic correlation. For wavefunctions which are eigenstates of the non-relativistic Hamiltonian, one can further distinguish linear combinations necessary to spin-adapt the N-electron function to a given $\langle S^2 \rangle$ value and those that are necessary for accuracy. A pre-adaptation of the reference functions to a given $\langle S^2 \rangle$ value by forming configuration state functions (CSFs) is also possible - in which case the CSFs other than the reference CSF would be said to constitute static correlation. On the other hand, dynamic correlation energy is the energy contribution of the large number of remaining determinants with small coefficients. The collective contribution of these determinants is often too significant to ignore. In our case, we shall see that both static and dynamic correlations are important.

The simplest ab initio electronic structure theory for excited states is the Configuration Interaction Singles (CIS)[15] theory. The lowest singlet and triplet excited state CSF's, formed by exciting an electron from orbital $i \rightarrow a$, in terms of Slater determinants $|\psi_i^a\rangle$, can be written as,

$$\begin{aligned} |^1\phi_i^a\rangle &= \frac{1}{\sqrt{2}}(|\psi_i^a\rangle + |\psi_i^{\bar{a}}\rangle) \\ |^3\phi_i^a\rangle &= \frac{1}{\sqrt{2}}(|\psi_i^a\rangle - |\psi_i^{\bar{a}}\rangle) \end{aligned} \tag{1}$$

The lowest eigenvalue of the difference of the S_1 and T_1 Hamiltonian matrices can be shown to be the lowest singlet-triplet gap ΔE_{ST} using Weyl's inequality in the following form[20],

$$\Delta E_{ST} = E_{S_1} - E_{T_1} = \lambda_{min}(^1H) + \lambda_{max}(^{-3}H) \geq \lambda_{min}(^1H - ^3H) \tag{2}$$

where,

$$({}^1H - {}^3H)_{ia,jb} = \langle {}^1\phi_i^a | H | {}^1\phi_j^b \rangle - \langle {}^3\phi_i^a | H | {}^3\phi_j^b \rangle = 2\langle \psi_i^a | H | \psi_j^{\bar{b}} \rangle = 2(ia||j\bar{b}) = 2(ia|jb) \quad (3)$$

This is simply twice of the conventional, antisymmetrized, two-electron exchange integrals in chemists' notation, which is known to be positive semidefinite[47]. Following the arguments in[20], its lowest eigenvalue, $\lambda_{min}({}^1H - {}^3H) \geq 0$ and $\Delta E_{ST} \geq 0$ for any CIS Hamiltonian. This implies that, within a single excitation framework (for an uncorrelated theory), this gap is always positive leading to a positive ST gap. It is also easy to see from here that since electron correlations typically lower the energies of electronic states and relatively higher amount of correlation in S_1 as compared to T_1 could, in principle, make the ST gap negative. In TD-DFT[18, 48, 49], electron correlations are accounted for through the exchange–correlation kernel, $f_{xc}(r, r', \omega)$ [50]. By analogy, we can also write a similar equation for TD-DFT (within the Tamn-Dancoff approximation),

$$\langle {}^1\phi_i^a | H | {}^1\phi_j^b \rangle - \langle {}^3\phi_i^a | H | {}^3\phi_j^b \rangle = 2(ia|jb) + 2(ia|f_{xc}^{\alpha,\beta}(r, r', \omega)|jb) \quad (4)$$

The exchange-correlation kernel $f_{xc}(r, r', \omega)$ is negative definite[50–52] leading to a reduction of the ST gap and ideally to inversion. But, for commonly known functionals this gap is always > 0 as sufficient correlation is not captured. It is well-known that TD-DFT fails to describe double excitations if a frequency-independent kernel is used (ie. under the adiabatic approximation)[49, 53]. On the other hand, double hybrid functionals[44] introduce double excitations through a post-SCF MP2 correction and can give an inverted ST gap[21, 24, 36]. We justify this in our forthcoming publication and compare various functionals through proper benchmarking[12]. An alternative path to obtain open-shell singlet excited states at the SCF level is to use a modified algorithm to converge to a higher state in a brute-force manner leading to the Δ SCF methods. There are several strategies for this with the most common ones being the maximum overlap method (MOM)[54], square-gradient minimization method (SGM)[55, 56], restricted open-shell Kohn-Sham (ROKS)[57], excited state DFT (e-DFT)[58] etc. However, the Δ SCF methods suffer from severe spin contamination mostly due to forceful representation of a multi-determinant wave-function as a single-determinant. Non-orthogonality of ground and excited state functions makes it very difficult to obtain transition properties. Thus, we believe that Δ SCF methods while cheap and convenient should be restricted to initial screening applications and not for detailed study. Correlation

methods such as MP2 and CCSD can also be applied on the optimized HF excited states leading to Δ MP2 and Δ CCSD excitation energies.

CIS(D) includes a perturbative doubles correction on the CIS excitation energies akin to MP2 giving size consistent energies as opposed to CISD. EOM-CCSD may be considered as the linear response of the CCSD ground state function. The EOM-CCSD excitation energies show an exact cancellation of the common correlation terms between the ground and excited states. The differential orbital relaxation is included up to linear terms but the differential correlation is not included under the SD truncation.

The most common starting point for a multireference theory[59] is the Multi-Configuration SCF (MCSCF). In the MCSCF approach, an active N-electron space needs to be defined. The selection is based on choosing a set of quasi-degenerate molecular orbitals or those that are the most relevant in describing the chemical bonding or the electronic excitations of interest. If the active electrons are distributed in all possible ways to make the model functions, a Complete Active Space (CAS) is created. The CASSCF[39] function for the k^{th} state is then written as:

$$|\psi_k\rangle = \sum_{\mu=1}^{n_{det}} |\phi_\mu\rangle c_{\mu k} = \sum_{\mu=1}^{n_{CSF}} |\Phi_\mu\rangle d_{\mu k} \forall k \quad (5)$$

The Complete active space (CAS) wavefunction is thus expressed as a linear combination of singly-, doubly-, triply-substituted, etc. Slater determinants, but with the excitation operator confined within the subset of the selected active orbitals.

$$|\Psi_{CAS}\rangle = \sum_M |\Psi_M\rangle = C_0 |\Psi_0\rangle + \sum_{i,a} C_i^a |\Psi_i^a\rangle + \sum_{ij,ab} C_{ij}^{ab} |\Psi_{ij}^{ab}\rangle + \sum_{ijk,abc} C_{ijk}^{abc} |\Psi_{ijk}^{abc}\rangle + \dots \quad (6)$$

Here C_i^a , C_{ij}^{ab} , C_{ijk}^{abc} , etc. are the corresponding coefficients of expansion, indicating singly, doubly, triply, etc. excited configurations respectively. The relative weights of the sums of square of C_{ij}^{ab} , C_{ijk}^{abc} , etc. coefficients reflects the importance of doubly, triply n-tuply excited states beyond the singly excited ones. Doubly excited configurations are thus explicitly present in the excited-state wave function and excited states with doubles character can be obtained with equal facility as those with dominance of singles unlike CIS, RPA and TD-DFT. The primary objective of CASSCF is to accurately describe the static electronic correlation. By allowing a flexible choice of active space, CASSCF can handle systems with significant static correlation, such as molecules in the bond-breaking or bond-forming regions as well as highly multireference excited states.

Inclusion of further dynamic correlation on top of the multireference function, can be carried out through perturbative[40, 60–65], CI-like[66] or CC-like[67–70] approaches. These constitute the family of multireference correlation theories which are called uncontracted if the ansatz for dynamic correlation excites out of the individual ϕ_μ and contracted if it excites directly out of the ψ_k [71]. In this paper we have selected Strongly-contracted N-Electron Valence Perturbation Theory Second Order (SC-NEVPT2)[40], Complete Active Space Perturbation Theory Second Order (CASPT2)[60, 61] and Fully Internally Contracted Multireference Configuration interaction singles-doubles (FIC-MRCISD)[66] as representative theories from the various classes of multireference correlation theories. The Internally Contracted Multireference Coupled Cluster (ICMRCC)[72] theory turned out to be too computationally expensive for these molecules in the chosen basis. All three belong to the contracted category.

NEVPT2[40] accounts for the dynamic correlation effects by considering the interaction between the active space and the remaining inactive orbitals and electrons in a perturbative manner. It is particularly useful for treating systems with moderately high dynamic correlation effects. FIC-MRCISD[66] (denoted as FIC-MRCI in this paper) is a non-perturbative diagonalization method that includes a larger number of configurations compared to NEVPT2 and a complete linear coupling between them, allowing it to capture a more extensive range of dynamic correlation effects. The FIC-MRCI is the best possible benchmark method for medium-sized highly correlated molecular systems such as in this current article and we shall use it as our benchmark theoretical method. It has predicted excitation energies and ST gaps consistent with experiments, which aligns with our theoretical expectations. The issue of size extensivity[73], which is lacking in FIC-MRCI, can be overlooked for excitation energy computations but for bond-breaking situations it becomes critical, and NEVPT2 and ICMRCC[72], which are fully size extensive would then be more reliable.

In the next sections we compare and analyze the performance of these theories in the context of predicting the S_1 - S_0 and T_1 - S_0 excitation energies and hence, the singlet-triplet gap (ΔE_{ST}) in a set of cyclazine-based templates shown in Fig. 1.

III. COMPUTATIONAL DETAILS

All CIS, CIS(D), RPA, RPA(D) and DLPNO-STEOM-CCSD calculations were performed using the ORCA 5.2.1 package[74]. All the EOM-CCSD, ADC(2) and Δ CCSD calculations using the Maximum Overlap Method (MOM)[54] are performed using a trial version of the Q-Chem 6.0.1 package[75]. The state average complete active space self consistent field (SA-CASSCF) calculations along with FIC-CASPT2, SC-NEVPT2 and FIC-MRCI are done in ORCA 5.2.1[74]. For the SA-CASSCF calculations two singlet states S_0 and S_1 and one triplet state T_1 has been averaged out. Alrich’s def2-TZVP basis set[76] has been used unless explicitly mentioned. For the Δ CCSD(T)[77, 78] calculations, the cc-pVDZ[79] basis set has been employed. The molecular geometries are optimized in ORCA using B3LYP[80]/def2-TZVP with Grimme’s D_3 dispersion corrections[81]. Vibrational frequency analyses were performed on all optimized geometries to confirm their nature as global minima. A tight SCF convergence criterion (10^{-8}) was fixed for all calculations. For a few cases among the Δ SCF methods, it was difficult to converge the S_1 state with the MOM strategy. In these cases we relaxed the convergence criterion to 10^{-6} . All the absolute values of state energies in atomic units (*au*) are reported in the Table. S1A and S1B of the supplementary material. The FIC-MRCISD and EOM-CCSD computations were the most computationally expensive methods with runtime on a single CPU of the order of 10-14 hours while all the DFT methods took less than half an hour for each run. We emphasize that the purpose of the state-of-the-art computations is to provide benchmark numbers for proper evaluation of cheaper methods and identification of necessary physics.

IV. RESULTS AND DISCUSSIONS

In this article, we have looked at the electronic structures of a set of three molecules (given in Fig 1) in their ground, S_1 , and T_1 states. Azine-1N and azine-4N are two of the very first compounds that were found to have inverted singlet-triplet gaps. The experiment determined the singlet-triplet gaps for azine-1N and azine-4N to be -0.07[1] and < 0.1 [2] eV, respectively. Recent theoretical investigations[20–22, 24, 25, 82] have also reported inverted ST gaps. Azine-7N or heptazine has been extensively researched in recent years for its theoretically predicted large inverted singlet-triplet gap of about -0.25 eV[20]. The HOMO

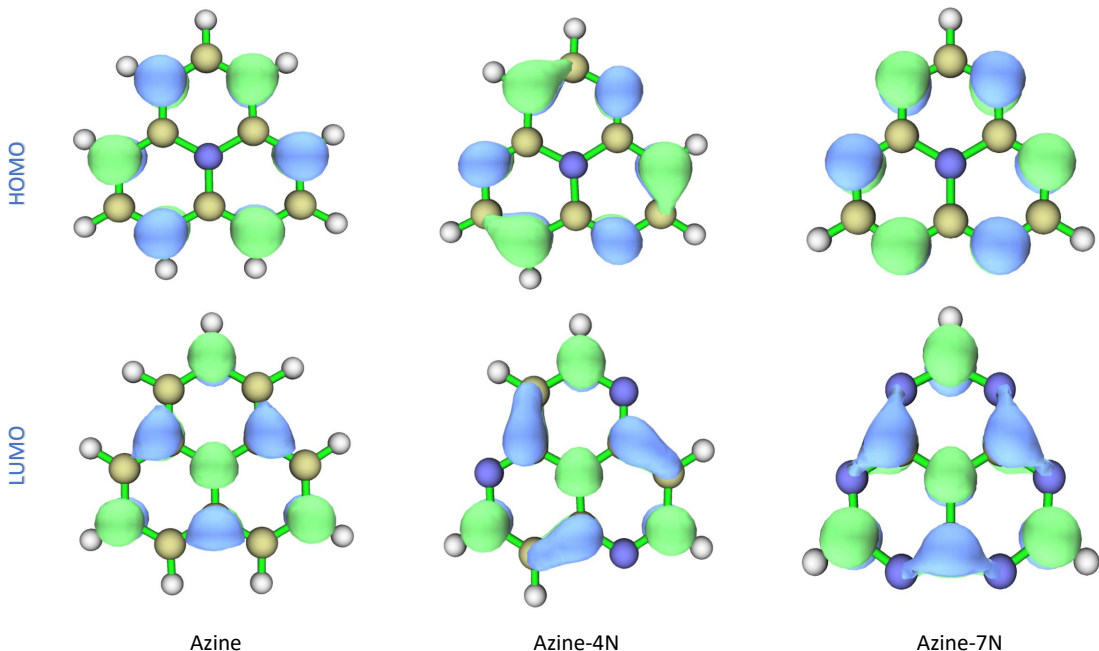


FIG. 3: HOMO-LUMO of three molecules in Fig. 1 with B3LYP/def2-TZVP level of theory

and LUMO of these molecules are given in Fig 3, with clearly visible spatially separated electron densities. This reveals the charge transfer (CT) character of the excited states in all three molecules[20] and indicates a suitability for OLED applications which has further fueled interest in these molecules. We can observe a reduction in radicaloid nature of the ground-state (S_0), from azine-1N to azine-7N, as indicated by the integrated number of electrons (N) housed on fractionally occupied orbitals (see Table S2 from supplementary material).

In the discussions that follow, we divide our work into two groups - single reference and multi-reference based methods. This helps us to disentangle the role of dynamic correlation and static correlation. It is most important to realize that the terminology of ‘doubles’, ‘triples’, etc. needs a qualifier indicating the reference function. Since the S_1 and T_1 states are primarily singly excited with respect to S_0 , many of the ‘doubles’ with respect to S_0 (which are the most important contributors to the dynamic correlation of S_0) are only ‘singles’ with respect to S_1 or T_1 . Conversely, the ‘doubles’ necessary to correlate S_1 and T_1 are ‘triples’ relative to S_0 . As the various correlated electronic structure methods include varying amounts of these excited functions, their suitability for different types of electronic

states differ. From a different perspective, the successes and failures of different methodologies gives us an insight into the nature of the electronic states under study. We also include a few selected DFT-based methods to emphasize our conclusions in this paper and present a thorough benchmark study in a paper to follow[12].

For these azine-xN (x=1,4,7) molecules, the most consistent description of their correlation that we have arrived at from a careful study of the comparative numbers is as follows. The S_0 state is single-reference but has a large amount of dynamic correlation. The S_1 state is multi-reference and is dominated by a singly excited configuration out of S_0 but contains significant contributions from doubles ($\approx 7\%$ for azine-1N) and triples ($\approx 1-2\%$ for azine-1N). The S_1 state has a large amount of dynamic correlation too but most of it comes from configurations common between the correlated S_0 and S_1 functions. The T_1 state, on the other hand, is also primarily singly excited with significant contributions from doubles ($\approx 5 - 6\%$ for azine-1N) but a larger triples contribution ($\approx 2 - 3\%$ for azine-1N) than S_1 . The dynamic correlation of T_1 come from configurations not common to those correlating S_0 . The most important correlation effect is the spin-dependent (or equivalently, state-specific) orbital relaxation in the presence of correlation. This is sometimes also called spin-polarization in more general terms. We justify the above assertions in the discussions that follow. In earlier publications, the dynamic correlation of S_1 has been the main focus and little attention has been paid to T_1 [20–22]. However, we have found in the course of our investigations that the S_1 - S_0 gap is far easier to model than the T_1 - S_0 gap. This confusion stems partly from the desire to obtain a large inversion of the S_1 and T_1 which comes about when S_1 is properly correlated, but T_1 is not, leading to a premature celebration of the success of the theories which invert the gap. A proper balanced treatment leads to near degeneracy in line with experiments. A similar conclusion has been reached by Dreuw and Hoffmann [26] both with respect to including more correlation as well as larger basis sets. They have also analyzed the nature of the S_1 and T_1 states in terms of entanglement entropy and the so-called natural transition orbital participation ratio.

A. Single-reference framework

All the results from single reference theories are presented in Table 1. As explained in Sec. II, in uncorrelated theories such as CIS and TD-HF, the ST gap is predicted to

TABLE I: Vertical excitation energies (in eV) using single-reference methods. Geometries are optimized at B3LYP/def2-TZVP level.

Molecule	Methods	S ₁	T ₁	ΔE_{ST}
Azine-1N	TDHF/RPA/def2-TZVP	1.639	0.993	0.646
	RPA(D)/def2-TZVP	0.909	1.503	-0.59
	CIS/def2-TZVP	1.791	1.451	0.340
	CIS(D)/def2-TZVP	1.036	1.317	-0.280
	EOM-CCSD/def2-TZVP	1.068	1.146	-0.077
	DLPNO-STEOM-CCSD/def2-TZVP	0.689	1.113	-0.42
	EOM-CCSD/cc-pVDZ	1.094	1.201	-0.107
	STEOM-CCSD/cc-pVDZ	0.592	1.091	-0.499
	DLPNO-STEOM-CCSD/cc-pVDZ	0.631	1.118	-0.487
	ADC(2)/def2-TZVP	1.036	1.215	-0.17
	ADC(2)/cc-pVTZ ^a	1.02	1.16	-0.14
	ADC(3)/cc-pVTZ ^a	0.81	0.87	-0.06
	CC3/aug-cc-pVTZ ^d	0.979	1.110	-0.131
	Δ HF/cc-pVDZ	1.012	-0.763	-1.775
	Δ MP2/cc-pVDZ	1.434	2.875	1.441
	Δ CCSD/cc-pVDZ	0.881	1.190	-0.309
	Δ CCSD(T)/cc-pVDZ	1.182	1.187	-0.005
	Δ HF/def2-TZVP	0.955	-0.028	-0.983
	Δ MP2/def2-TZVP	1.423	2.958	1.535
	Δ CCSD/def2-TZVP	0.834	1.139	-0.305
	Δ CCSD(T)/cc-pVTZ ^a	-	-	0.025
	Δ CCSD(T)/aug-cc-pVTZ ^a	-	-	0.029
	Expt ^b	0.97	0.93/1.05	0.04/-0.07
Azine-4N	TDHF/RPA/def2-TZVP	3.163	1.188	1.975
	RPA(D)/def2-TZVP	2.141	3.872	-1.731
	CIS/def2-TZVP	3.297	2.526	0.771
	CIS(D)/def2-TZVP	2.226	2.474	-0.248
	EOM-CCSD/def2-TZVP	2.382	2.213	0.169
	DLPNO-STEOM-CCSD/def2-TZVP	1.889	2.082	-0.193
	ADC(2)/def2-TZVP	2.147	2.138	0.009
	Expt ^c	<2.39	2.29	<0.1
	Azine-7N	TDHF/RPA/def2-TZVP	4.243	3.671
RPA(D)/def2-TZVP		2.494	3.104	-0.61
CIS/def2-TZVP		4.351	3.94	0.411
CIS(D)/def2-TZVP		2.649	3.172	-0.523
EOM-CCSD/def2-TZVP		2.916	3.066	-0.150
DLPNO-STEOM-CCSD/def2-TZVP		2.297	3.531	-1.234
ADC(2)/def2-TZVP		2.668029	2.916	-0.248
ADC(3)/cc-pVTZ ^a		2.81	2.88	-0.07
CC3/aug-cc-pVTZ ^d		2.717	2.936	-0.219
Expt ^e		<2.39	2.29	<0.1

be positive. When doubly excited configurations are included in any way, the situation is drastically altered. The gap is predicted to be negative by the various correlated wave function-based approaches, CIS(D), ADC(2), EOM-CCSD, DLPNO-STEOM-CCSD and RPA(D) although they do not all quantitatively agree. CIS(D), ADC(2) and EOM-CCSD approach the experimental S_1 - S_0 gap (and also our theoretical benchmark FIC-MRCI (12,9)) to within approximately 0.1 eV for all three molecules) but the T_1 - S_0 gap turns out to be more challenging. RPA(D) and CIS(D) give a too high value but a full canonical EOM-CCSD (1.146 eV for azine-1N) is reasonable. Our comparison between EOM-CCSD and STEOM-CCSD for azine-1N shows that the similarity transformed EOM (STEOM) approximation is not reliable for this type of molecules. We must point out that the DLPNO-STEOM-CCSD method has been used as a benchmark in certain recent publications leading to confusion regarding the relative accuracy of various methods[21, 82]. Coming to the ADC-based methods, ADC(2) performs reasonably well in the def2-TZVP basis chosen by us but a comparison between ADC(2)/cc-pVTZ and ADC(3)/cc-pVTZ from Ref[26] shows a deterioration of individual excitation energy values although the accuracy of the gap is maintained by error cancellation. The Δ CCSD and Δ CCSD(T) numbers adapted from Ref[26] and our own computations in the cc-pVDZ basis set show that both energy gaps are poorly described by Δ CCSD relative to EOM-CCSD but the triples (T) push them in the right direction again. We justify all these observations in the next few paragraphs.

CIS(D) and EOM-CCSD include a set of doubles on S_0 . The contribution of these doubles is estimated in an MP2-like state-specific fashion for CIS(D) and with the CCSD method in EOM-CCSD. Needless to say, the CCSD method includes more dynamic correlation than the (D) method but clearly the error cancellation between S_1 and S_0 is good unlike that for S_0 and T_1 . Double excitations in the S_0 and S_1 states are thought to contribute about 10%, according to the amplitudes of the CIS(D), EOM-CCSD and ADC(2) wave functions. Now, for the T_1 state, CIS(D) is not able to include sufficient dynamic correlation as we have discussed above. The S_1 and T_1 states (of azine-1N, for example) have about 5 – 7% of doubly excited configurations with respect to S_0 (which are mostly singles out of their respective reference functions) if one were to allow a multireference description (see Fig. 6). The dynamic correlation of these configurations cannot be accounted for in a single-reference SD framework but can be included with triples (or alternately, with doubles out of a multi-reference function). Hence, the triples in the Δ CCSD(T) make-up for the lack of inclusion

of other singly-excited configurations in the reference function.

The ADC manifold of excited state theories performs better in estimating the ΔE_{ST} than the individual excitation energies presumably due to error cancellations correct to a certain order of perturbation. In ADC(2) for instance, the ground state and all excited states are obtained correct up to second order of perturbation. The Hilbert space covered by ADC(2) and ADC(3) are same as CIS(D) but the balancing act in the coupling terms between the various excitation sub-spaces predicts more accurate excitation energies through error cancellation. ADC(3) shows an improvement in ΔE_{ST} with MP3 level ground and excited states. This behaviour is similar to that of CASSCF with smaller active spaces as can be seen in Table. S3 from the supplementary material.

The Δ CC methods apply a CCSD ansatz on the Hartree-Fock function of the chosen state. For the S_1 state this can be obtained by a maximum-overlap algorithm[54] when computing the reference Hartree-Fock state, for instance, while S_0 and T_1 are the variational minima of their respective spin multiplicities. The UHF numbers (of azine-1N, for example) from the supplementary material indicates that the energy of the MOM-UHF for S_1 is very close to S_0 but with an $\langle S^2 \rangle$ value of 2.01, while T_1 has $\langle S^2 \rangle = 2.49$. Spin contamination of S_1 is thus, larger than T_1 . Δ HF underestimates the $S_1 - S_0$ gap but is reasonable for the $T_1 - S_0$ gap leading to a large negative ΔE_{ST} -0.98 eV. On the other hand, Δ MP2 gives a large positive ΔE_{ST} due to overestimating both the $S_1 - S_0$ and $T_1 - S_0$ excitation energies. However orbital optimized (OO)-MP2 is able to predict the $T_1 - S_0$ gap (1.02 eV at OO-MP2/def2-TZVP) quite accurately recovering the spin of the T_1 state with a $\langle S^2 \rangle$ value of 2.01. Incidentally spin-opposite scaling (SOS) correction to OO-MP2 has a poorer outcome of 1.26 eV as expected.

The Δ CCSD method has the additional limitation of the absence of error cancellation (a strength of linear response methods) which makes it all the more crucial to include all of the correlation. UCCSD on the spin broken UHF references improves the $\langle S^2 \rangle$ [83] (from 2.29 (UHF/cc-pVDZ) for the T_1 to 2.014 (UCCSD/cc-pVDZ) in azine-1N reported in ref[26]) , but the ΔE_{ST} result is still very poor due to the spin contamination of S_1 ($\langle S^2 \rangle = 1.042$). It is interesting to note that the UHF-CCSD/cc-pVDZ computation for the T_1 state of azine-1N which has the almost correct $\langle S^2 \rangle$ value of 2.014 (ideally $\langle S^2 \rangle = 2$) also shows an accurate $T_1 - S_0$ energy of 1.19 eV (EOM-CCSD/cc-pVDZ, $E_{T_1} = 1.201$ eV and ROHF-CCSD/cc-pVDZ, $E_{T_1} = 1.19$ eV). One may thus attribute the failure of the Δ CCSD method

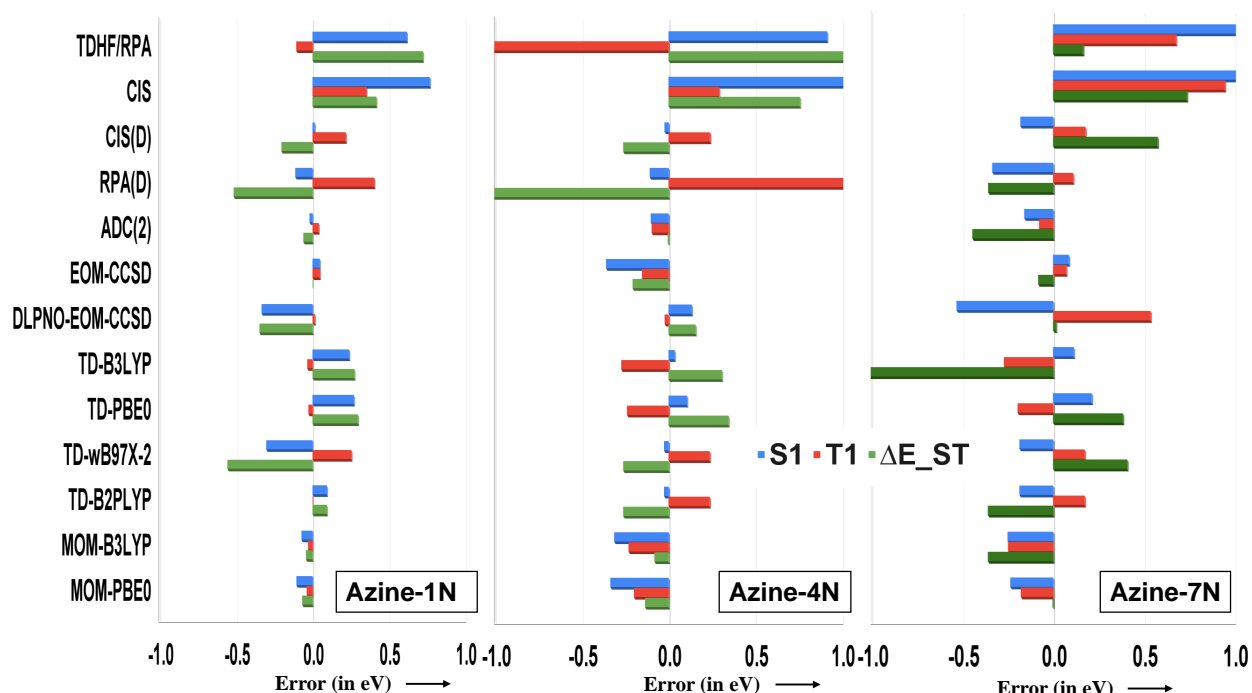


FIG. 4: Differences in the S_1-S_0 , T_1-S_0 and ΔE_{ST} energy values in eV for Azine-1N, Azine-4N and Azine-7N computed with various single-reference correlation theories with FICMRCI (12,9) as the benchmark value

to the spin-contamination of the reference determinant and the deficiencies of the reference function. Remarkably, in the UCCSD(T)[77, 78] the inclusion of the triples, (T), improves the energy differences greatly presumably due to the correction of the spin contamination along with the need to make up for the partial multireference nature of the reference function as discussed earlier.

On the other hand, the ROSGM[57] formalism for HF, MP2 and CCSD uses a spin pure reference determinant resulting in excited SCF states that are orthogonal. We have seen that ΔE_{ST} values for ROSGM-HF are always positive (contrary to the MOM-UHF). But ROSGM-MP2 erroneously leads to a large negative ST gap. ROSGM-CCSD subsequently recovers values close to UHF-CCSD for the T_1 state possibly through introduction of sufficient correlation and some degree of spin contamination from the non-linear unrestricted ansatz. The S_1 excitation energies continue to be poor for ROSGM-CCSD leading to a large positive ΔE_{ST} .

In Fig. 4 we plot the excitation energies and ΔE_{ST} for azine-1N, azine-4N and azine-7N respectively computed with various single reference theories and also present some popu-

lar density-based methods for comparison and additional insight. Interestingly, using the traditional LR-TDDFT technique with standard exchange-correlation functionals, positive singlet-triplet gaps ($\Delta E_{ST} > 0$) are obtained but through a Δ SCF approach such as the maximum overlap method (MOM)[54] a negative ST gap is obtained for the same XC functionals (eg. B3LYP and PBE0). This identifies the cause of the failure of LR-TDDFT for inverted singlet-triplet gaps as the absence of state-specific correlation coupled with orbital optimisation in the excited states which the MOM technique can capture. By introducing spin-breaking in the KS determinant, we mimic part of the effect of spin-polarization[84] but in an uncontrolled manner. We believe that the good performance of MOM-based DFT methods lies in introducing the spin-polarization through a coupling with the exchange-correlation functionals rather than the spin-breaking itself, similar to that observed in OO-MP2 for the T_1 state.

In fact, removing the spin-contamination, through adopting, for example ROKS formalism[57] one is back to positive ST gaps[85] (eg. UB3LYP gives ST gap -0.12 eV with $\langle S^2 \rangle$ value 1.09 and 2.011 for S_1 , T_1 , while ROKS-B3LYP gives ST gap 0.13 eV). The only difference here is the $\langle S^2 \rangle$ value (spin-contamination) clearly indicating its role in inversion of the ST gap during state specific orbital optimization. We must also note that MOM-DFT methods are much less spin-contaminated than UHF and KS orbitals have recently been adopted for post-SCF computations based on this argument[86–89]. There are other strategies within DFT to include orbital orbital relaxation effects in the variational excited state solutions[55–57] which have a comparable performance vis a vis the MOM approach. Adding additional correlation through a post-KS-TDDFT state-specific MP2-like correction to the excited state energies in the so-called double hybrid XC functional based TD-DFT also captures the inversion[21, 36, 90]. Among the various double hybrid functionals ω B97X-2 appears to perform poorly across all molecules. The others we have studied have similar and low errors. We try to understand this further along with the success of the Kohn-Sham Δ SCF methods using a larger test set of molecules in a forthcoming partner publication[12]. We do not expect quantitative accuracy from KS-DFT but rather a consistent protocol for screening a large number of molecules.

In this section we have seen that inclusion of dynamic correlation through single reference correlated wave function based methods - CIS(D), ADC(2) or EOM-CCSD, Δ CCSD or Δ SCF approaches through DFT, is sufficient to obtain inverted singlet-triplet ordering.

However, the accurate estimation of the singlet-triplet near degeneracy seen in experiments is only achieved in EOM-CCSD and Δ CCSD(T) indicating the need for either including static correlation or somehow balancing the amount of dynamic correlation in the states involved. Spin polarization through correlation is possibly the dominant physical effect that needs to be captured. The average D_1 diagnostics[91] value for the S_1 state of the three systems at the CC2 level (as reported in[22]), is 0.08, which are marginally greater than the $D_1 \leq 0.05$ criterion for single-reference character. The (GS) T_1 -diagnostic[92] for azine-7N yields a value of 0.02 at CCSD/aug-cc-pVTZ level as reported in[31], indicating absence of multi-reference (MR) character. Furthermore, % T_1 values of 86.3% and 95.7% are reported[31] for the lowest excited singlet and triplet states, respectively, from CC3/aug-cc-pVDZ computations. This indicates dominance of singly excited character but the S_1 state has a significant contribution from doubly excited configurations. The lack of full orbital relaxation in the CCSD function (since the CC ansatz only modifies the ket function) can also lead to different conclusions of excitation character from CC-based and CASSCF based methods. In any case, to further understand the relative weights of various configurations in these states we continue our investigations with a suite of multi-reference correlation theories in the next section.

B. Multi-reference framework

For the multi-reference treatment of any electronic state, a proper choice of ‘active space’ is necessary. As discussed in Sec. II, this involves choosing a set of ‘active orbitals’ from a previous single-reference SCF computation. The active orbitals need to be chosen through experience and intuition as no definite rule is available. Guidelines and automated tools for active space selection are a field of ongoing research[93–95]. There are roughly-speaking two common practices - energy based and phenomenon based - although several new strategies are recently being investigated[96, 97]. In the energy-based strategy one selects quasi-degenerate orbitals from among the occupied and unoccupied molecular orbitals (MOs). This becomes progressively difficult as the size of the molecule increases and a clear cut-off cannot be obtained in the orbital energies. Moreover, the success of this strategy depends very much on the quality of the MOs in the starting calculation. In the phenomenon-based strategy one may choose the orbitals involved in a bond-breaking process as the active or-

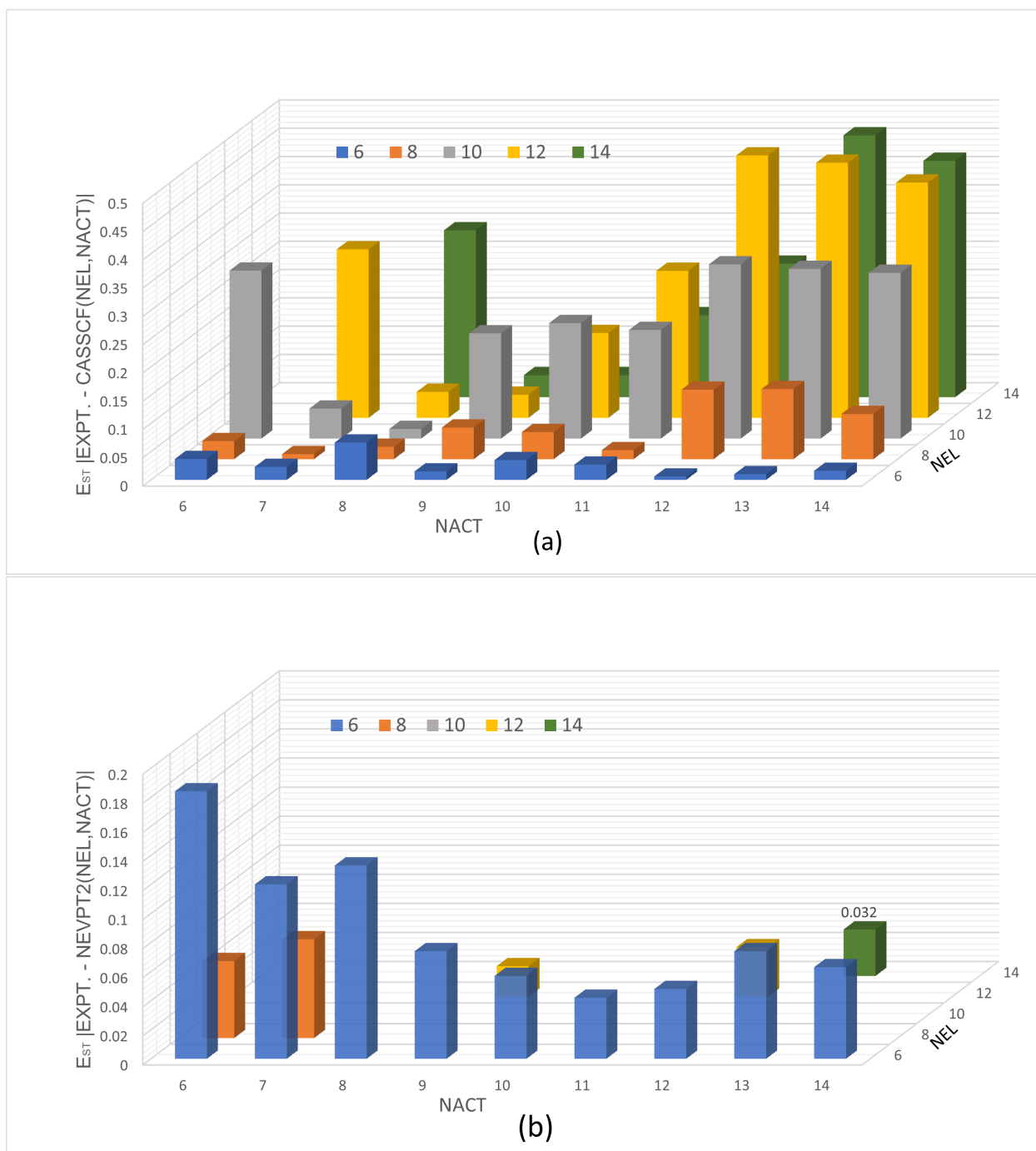


FIG. 5: Deviation of CASSCF results with experimental value (in eV) for varying active space and NEVPT2 values for selected active space for azine-1N

bitals for constructing a potential energy curve or, as in our case, the class of orbitals likely to be involved in a particular type of excitation. Since the Hartree-Fock reference function is qualitatively wrong in our case, we have carried out a thorough study of the possible active spaces before arriving at the correct choice for further correlation studies. We discuss this

below.

In Table S3 in the supplementary material we report the excitation energies and ST gaps of azine-1N computed using CASSCF with various choices of active electron (N_{el}) and active orbitals (N_{act}) chosen in energy ordering (with a plot of the values in the Fig S2). The errors in the ΔE_{ST} against the experimental value of -0.07 eV of azine-1N along with NEVPT2 error plot for selected active spaces are presented in the segment (a) and (b) of Fig. 5 respectively. It is evident from the values, that a naive increase of active orbitals and electrons does not help in finding the correct active space. The lack of convergence of the CASSCF excitation energies with increasing active space can be an indication of poor starting orbitals and/or significant dynamic correlation[96]. From a phenomenon-based point of view, all π and π^* orbitals from the RHF calculation of azine-1N should be considered as active orbitals along with the lone pair orbital of N. For azine-1N there are 6 π bonds and 1 lone pair orbitals which are occupied and 6 π^* and 1 or more N p_z containing unoccupied orbitals. The 6 π orbitals from HOMO-5 to HOMO and 3 π^* valence orbitals, LUMO to LUMO+2, are energetically in order and can be included in a CAS(12,9) (12 electrons, 9 orbitals) calculation. The rest are reshuffled in the RHF calculation. Beyond the (12,9) space, we have identified the N lone pair and reshuffled the orbitals to form the (14,10) CAS. Subsequently, we identified all the likely unoccupied active orbitals and did a systematic increase of active space for only one case (azine-1N) upto a CAS(14,14) which is the largest active space we have considered. These results are presented in Table S5 in the supplementary material. In the same table, we also present the excitation energies after inclusion of dynamic correlation on these active spaces. This is important to compare because for the smaller active spaces such as (6,n) or (8,n), etc which do not have any logical basis for being a good choice, there is an apparent accuracy in the energy values at the CASSCF level (Fig. 5(a)). But, further inclusion of correlation distorts the picture indicating that the agreement was fortuitous as borne out by the NEVPT2 error plot in the Fig. 5(b). The inclusion of the N lone pair orbital led to marginal improvement in azine-1N. Inclusion of the remaining π^* s which are energetically even higher than some σ^* orbitals led to a deterioration of the results presumably due to the poor quality of the HF MOs. To cross-check our reasoning, we have carried out CASSCF (14,10) computations using a reference determinant constructed using CASSCF (14,14) orbitals (see Table S5 of the supplementary material). There is a marked improvement in this case taking the excitation energies closer

to the FIC-MRCI (14,10) values. We may thus assert that a significant portion of the role of post-CASSCF corrections comes from state-specific orbital relaxation. This is also an indirect argument for the success of Δ SCF DFT methods using MOM/SGM techniques (see Fig (4)). In summary, CAS(12,9) where 6 occupied π and 3 virtual π^* are included appears to be a good choice as it satisfies both the energetic criteria and the phenomenon-based criteria in the active space. In the case of the other systems, the RHF computation gives rise to 3 occupied π and 3 virtual π^* orbitals ordered energetically while the other π and π^* orbitals are reshuffled. Including other π orbitals through swapping we have extended the active space to (12,9) and then to (14,10) by including N-lone pair. Pictures of the active orbitals taken for the CAS(12,9) and CAS(14,10) CASSCF calculations are presented in Fig. S1 of the supplementary material along with the natural occupation numbers of the fractionally occupied active orbitals for state-specific CASSCF(12,9) calculations for S_0 , S_1 and T_1 states in Table S2. Errors in all the multi-reference theories against the experimental values for azine-1N with different active spaces are plotted in Fig. S5 in the supplementary material.

To further understand the nature of the static correlation, we have studied the weightage of double- and higher-order excitations in the final CAS wavefunction of these systems. However, while evaluating the double excitation character of the S_1 state, the multi-reference nature of the ground state must be taken into consideration. Thus we refer to the RHF function of the S_0 state as the reference determinant for classifying singles, doubles, triples, etc. In the following discussion we generally refer to the computation with a (12,9) CAS but the corresponding values for the (14,10) CAS are also presented in Fig. 6. For all the molecules, the HF configuration makes up about 90% of the ground-state CASSCF wave function but it also contains a significant contribution (5%) from the doubly excited configurations. With singly excited configurations contributing between 80% - 87%, the S_1 and T_1 excited state is primarily singly excited in nature with the largest contribution coming from a single CSF. The multi-reference nature of S_1 and T_1 comes from the doubles which contribute 5 - 7% and triples which contribute 1 - 2%. On comparing the CASSCF configurations of the (12,9) and (14,10) active spaces, no significant new configurations are seen. However, the T_1-S_0 excitation energy reduces by 0.012 eV indicating partial inclusion of dynamic correlation rather than static correlation. The weightage of the singles, doubles and triples contributions in the CASSCF wave functions for the two different CAS spaces are

pictorially given in Fig. 6. If we consider the importance of n-tuple excitons beyond single-particle ones, it should be noted that values of 5%, 3%, and 3% for azine-1N, azine-4N, and azine-7N, respectively, are estimated for the S_0 wavefunction. For the corresponding S_1 (T_1) excited-states, these weights of the doubles are about 6 – 7% (5 – 6%) respectively. Given that Coulomb correlation predominantly involves the interaction between anti-parallel spins, it is known that doubly-excited configurations result in stabilisations that are a few times bigger for singlet than for triplet excited-states. This leads to greater relative lowering of the S_1 – S_0 gap vis a vis the T_1 – S_0 gap. In short, ground state of these molecules are predominantly single-reference (as evident from the (GS) T_1 diagnostic value[31]), S_1 and T_1 have moderate multi-reference character.

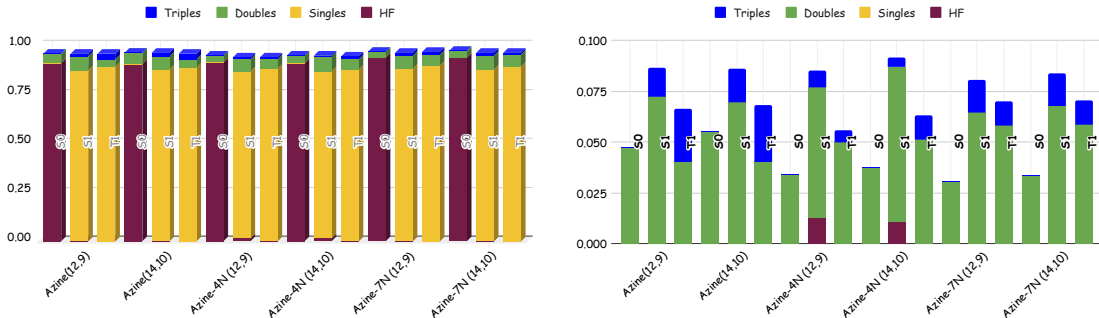


FIG. 6: Fraction of n-tuple excitations in CASSCF wavefunction of Azine-1N, Azine-4N and Azine-7N. The right-panel highlights the non-singles contribution to each state.

We have included dynamic correlation on the CASSCF wave-function, along with the PT2 methods - SC-NEVPT2 and FIC-CASPT2 and also the non-perturbative FIC-MRCI. SC-NEVPT2 predicts that the singlet-triplet gaps of all molecules would either be negative or very near to zero similar to EOM-CCSD. In all cases FIC-CASPT2 underestimates the energy gap. As shown in Table. S5 in the supplementary material, the CASSCF values are very poor for large active spaces even for (14,14) where all $\pi - \pi^*$ orbitals are considered. It indicates that the introduction of non-dynamical correlation effects is only a first step in dealing with the complex electronic effects of triangle-shaped systems. We can also see in Table S5, that NEVPT2 can recover a reasonable ΔE_{ST} from extremely poor CAS(12,12) and CAS(14,13) CASSCF values. This supports our suggestion that a static+dynamic correlation approach is less sensitive to the choice of the active space. Incidentally CASPT2 improves with increase in size of the active space. SC-NEVPT2, FIC-CASPT2 and FIC-

MRCI results are given in Table II for two different active spaces - CAS (12,9) and (14,10). The SA-CASSCF results for the S_1 and T_1 excitation energies of azine-7N are significantly reduced by the SC-NEVPT2 correction, yielding remarkably consistent results in all situations. Also take note of the quantitative agreement between SC-NEVPT2 values and experimental estimates for specific S_1 and T_1 excitation energies (which have been previously reported by benchmark calculations of tiny systems against pseudo-FCI[98]). It can be noted that for all cases, FIC-CASPT2 values are poor for selected active spaces and sometimes underestimates the exciton energies. But it is evident from the Table S5 of the supplementary material that, inclusion of more π^* orbitals beyond (14,10) CAS, leads to error in NEVPT2, but improves CASPT2 values. Infact, in the case of CAS(14,14), the FIC-CASPT2 value is very accurate and close to the experimental value. It is also reflected in the plot of the values presented in Fig. S5.

The FIC-MRCI includes a greater degree of dynamic correlation. From the FIC-MRCI results given in Table II for CAS (12,9) and (14,10), we can conclude that the S_1 and T_1 excitons significantly differ sometimes from the SC-NEVPT2 values. The dynamic correlation contributions to the excited state energies recovered through FIC-MRCI framework are about 10.24%, 1.9% and 6% in S_1 state for azine-1N, azine-4N and azine-7N respectively and 15%, 1% and 4.9% for the T_1 states. The percentage contribution of dynamic correlations captured by both the frameworks are similar for azine-1N, but deviate a lot for azine-4N and azine-7N. This indicates that these two molecules have large dynamical correlations.

We may thus opine that a benchmark method for this class of molecules should involve both static and dynamic correlation such as SC-NEVPT2 or FIC-MRCI such that the description of correlation is complete and hence, reliable across different molecules alongwith the advantage of less sensitivity to the choice of the active space (compared to CASSCF). EOM-CCSD is also quite good for the molecules studied here but from a theoretical perspective it misses the differential correlation of ground and excited states and may lead to reduced accuracy in other molecules.

V. SUMMARY AND FUTURE OUTLOOK

The lowest singlet S_1 and triplet T_1 excited states of a group of N-doped (triangular-shaped) -conjugated hydrocarbons, namely azine-1N, azine-4N, and azine-7N, are examined

TABLE II: Vertical excitation energies (in eV) for CAS(12,9) and CAS(14,10) with SC-NEVPT2, FIC-CASPT2 and FIC-MRCI. Geometries are optimized at B3LYP/def2-TZVP level.

Molecule	Method	CAS(12,9)			CAS(14,10)		
		S ₁	T ₁	ΔE_{ST}	S ₁	T ₁	ΔE_{ST}
Azine-1N	CASSCF	0.927	0.956	-0.029	0.974	1.005	-0.031
	NEVPT2	0.964	1.055	-0.091	0.939	1.043	-0.104
	CASPT2	0.413	0.656	-0.243	0.357	0.618	-0.261
	FICMRCI	1.022	1.099	-0.077	1.034	1.118	-0.084
	Expt ^b	0.97	0.93/1.05	0.04/-0.07	0.97	0.93/1.05	0.04/-0.07
Azine-4N	CASSCF	2.212	2.191	0.021	2.288	2.276	0.012
	NEVPT2	2.246	2.231	0.015	2.27	2.256	0.014
	CASPT2	1.585	1.71	-0.125	1.611	1.72	-0.109
	FICMRCI	2.249	2.235	0.014	2.301	2.294	0.007
	Expt	<2.39	2.29	<0.1	<2.39	2.29	<0.1
Azine-7N	CASSCF	2.841	2.999	-0.158	2.992	3.124	-0.132
	NEVPT2	2.59	2.77	-0.18	2.504	2.776	-0.272
	CASPT2	1.812	2.234	-0.422	1.715	2.202	-0.487
	FICMRCI	2.829	2.994	-0.165	2.9	3.097	-0.197
	Expt	--	--	<0	--	--	<0

for their energy ordering. In these systems the S₁–T₁ gaps are predicted to be negative, which will encourage exoergic reverse intersystem crossing events, which are useful in various optical device technologies such as OLEDs. Regardless of the exchange-correlation functional selected, the S₁–T₁ gap is always found to be positive when using the TD-DFT approach with standard exchange-correlation functionals. However, with the logical exception of CIS, every correlated wave-function approach investigated, such as CIS(D), EOM-CCSD, ADC(2), CASSCF, SC-NEVPT2, and FIC-MRCI resulted in $\Delta E_{ST} \leq 0$ values for these systems.

While most previous studies have focused on which methods predict a larger inversion, we have found that higher levels of theory actually predict near degeneracy of S₁ and T₁

with $-0.2 < \Delta E_{ST} < 0.01$ eV which is closer to experimental values where available. This is heartening because a large negative energy gap can also be detrimental to an efficient reverse intersystem crossing[10]. We have identified the delicate balance between static and dynamic correlation which takes us from the large positive ΔE_{ST} of uncorrelated wavefunction theories to the large negative ΔE_{ST} of CIS(D) and RPA(D) to the near degeneracy of EOM-CCSD, CASSCF, NEVPT2 and FIC-MRCI. A careful consideration of the CASSCF coefficients have indicated that while S_0 is single-reference, the S_1 and T_1 states are moderately multi-reference with about 5-15% contributions from configurations other than the reference for the respective states of the three molecules. The effect of these additional configurations can thus, be captured with a large amount of dynamical correlation or with a static plus dynamic approach. We have observed that the correlation of the T_1 state is only slightly weaker (not dramatic as surmised by others) than that of the S_1 which brings the state closer with a small inverted or near-zero gap. This difference is likely to arise from spin-dependent orbital relaxation and spin-dependent correlation relaxation[84]. Theories which capture the latter effects properly are found to give the most accurate results. In EOM-CCSD, the so-called R operators introduce spin-polarization of reference orbitals in the presence of correlation (from the T operators) within the single-reference framework. This coupling is absent in CIS(D) and RPA(D), for instance, which only include correlation additively. In CASSCF-based multireference approaches, on the other hand, correlation is included individually on spin-adapted references leading to automatic inclusion of these effects. One must note that while smaller active spaces in CASSCF sometimes give accurate numbers, subsequent inclusion of dynamic correlation may distort the trends leading to our suggestion of the (12,9) active space as being numerically accurate as well as being physically meaningful.

We have also explored the possibility of computing the singlet-triplet energies of our test set using the Δ SCF and Δ CCSD class of methods in order to observe the impact of state-specific orbital optimisation on the excited-state energetics. Our findings indicate that spin-contamination of the open-shell states play a very important role and can completely overshadow any gains from inclusion of state-dependent orbital optimization and correlation. This class of molecules show a very high spin contamination at the UHF level even for the T_1 state and subsequent inclusion of dynamic correlation through CCSD improves it but accurate numbers can only be achieved at the CCSD(T)[78] level. On the other hand,

UDFT methods show very little (if any) spin contamination for the variational minima states but significant spin-contamination is seen for the artificially converged higher excited states. However, this is still lower than that in the corresponding UHF excited state. Preliminary investigations indicate that Δ SCF DFT methods do very well for these molecules and we shall follow up with a more extensive benchmark study of DFT-based methods. These findings point to the necessity of spin-dependent correlation-sensitive orbital optimisation, which the LR-TDDFT lacks, in order to achieve accurate singlet-triplet gaps in these compounds. We have also found that the TDDFT(D) approach and the appropriate double-hybrid density functionals perform well.

Thus, this paper identifies the nature of the electron correlations which affect the lowest excitation energies of molecular templates for potential OLED materials and tries to explain the success and failure of various wavefunction-based ab initio electronic structure theories for computing inverted or nearly degenerate S_1 and T_1 excited states. EOM-CCSD, FIC-NEVPT2 and FIC-MRCISD have been found to be suitable benchmark methods. The density-functional approaches are to be discussed and benchmarked in a follow-up study such that one or more accurate yet computationally cheap theories can be identified for screening relatives and derivatives of the templates studied here.

Supporting Information

State energies of S_0 , S_1 and T_1 for azine-xN along with the cartesian geometries and pictures of the active orbitals used are recorded. Data from additional studies using multi-reference methods discussed in the paper are presented along with some plots to support the arguments in the paper.

Acknowledgements

SS gratefully acknowledges funding support from DST SERB, New Delhi, India (SRG/2021/000737) and IISER Kolkata. SC want to thank IISER Kolkata for Junior Research Fellowship. Prof. Ashwani K. Tiwari is acknowledged for sharing his computational

facilities. We thank the two anonymous referees for their valuable comments.

- [1] Leupin, W.; Wirz, J. Low-Lying Electronically Excited States of Cycl[3.3.3]azine, a Bridged 12π -Perimeter. *J. Am. Chem. Soc.* **1980**, *102*, 6068.
- [2] Leupin, W.; Magde, D.; Persy, G.; Wirz, J. 1, 4, 7-Triazacycl [3.3. 3] azine: basicity, photoelectron spectrum, photophysical properties. *J. Am. Chem. Soc.* **1986**, *108*, 17.
- [3] Endo, A.; Sato, K.; Yoshimura, K.; Kai, T.; Kawada, A.; Miyazaki, H.; Adachi, C. Efficient up-conversion of triplet excitons into a singlet state and its application for organic light emitting diodes. *Appl. Phys. Lett.* **2011**, *98*, 083302.
- [4] Uoyama, H.; Goushi, K.; Shizu, K.; Nomura, H.; Adachi, C. Highly efficient organic light-emitting diodes from delayed fluorescence. *Nature* **2012**, *492*, 234.
- [5] de Silva, P.; Kim, C. A.; Zhu, T.; Van Voorhis, T. Extracting design principles for efficient thermally activated delayed fluorescence (TADF) from a simple four-state model. *Chem. Mater.* **2019**, *31*, 6995.
- [6] Difley, S.; Beljonne, D.; Van Voorhis, T. On the singlet-triplet splitting of geminate electron-hole pairs in organic semiconductors. *J. Am. Chem. Soc.* **2008**, *130*, 3420.
- [7] Sato, T.; Uejima, M.; Tanaka, K.; Kaji, H.; Adachi, C. A light-emitting mechanism for organic light-emitting diodes: Molecular design for inverted singlet-triplet structure and symmetry-controlled thermally activated delayed fluorescence. *J. Mater. Chem. C* **2015**, *3*, 870.
- [8] Di, D.; Romanov, A. S.; Yang, L.; Richter, J. M.; Rivett, J. P. H.; Jones, S.; Thomas, T. H.; Abdi Jalebi, M.; Friend, R. H.; Linnolahti, M. High-performance light-emitting diodes based on carbene-metal-amides. *Science* **2017**, *356*, 159.
- [9] Olivier, Y.; Sancho-García, J. C.; Muccioli, L.; D’Avino, G.; Beljonne, D. Computational Design of Thermally Activated Delayed Fluorescence Materials: The Challenges Ahead. *J. Phys. Chem. Lett.* **2018**, *9*, 6149.
- [10] Dinkelbach, F.; Bracker, M.; Kleinschmidt, M.; Marian, C. M. Large Inverted Singlet–Triplet Energy Gaps Are Not Always Favorable for Triplet Harvesting: Vibronic Coupling Drives the (Reverse) Intersystem Crossing in Heptazine Derivatives. *J. Phys. Chem. A* **2021**, *125*, 10044.
- [11] Aizawa, N.; Pu, Y.-J.; Harabuchi, Y.; Nihonyanagi, A.; Ibuka, R.; Inuzuka, H.; Dhara, B.; Koyama, Y.; Nakayama, K.-i.; Maeda, S.; Araoka, F.; Miyajima, D. Delayed fluorescence from

- inverted singlet and triplet excited states. *Nature* **2022**, *609*, 502–506.
- [12] Chanda, S.; Saha, S.; Sen, S. Benchmark Computations of Nearly Degenerate Singlet and Triplet states of N-heterocyclic Chromophores: II. Density-based Methods. *To be submitted* **2024**,
- [13] Hund, F. Zur deutung verwickelter spektren, insbesondere der elemente scandium bis nickel. *Physik* **1925**, *33*, 345.
- [14] Bene, J. E. D.; Ditchfield, R.; Pople, J. A. Self-Consistent Molecular Orbital Methods. X. Molecular Orbital Studies of Excited States with Minimal and Extended Basis Sets. *J. Chem. Phys.* **1971**, *55*, 2236–2241.
- [15] Foresman, J. B.; Head-Gordon, M.; Pople, J. A.; Frisch, M. J. Toward a systematic molecular orbital theory for excited states. *J Phys. Chem.* **1992**, *96*, 135–149.
- [16] Bouman, T. D.; Hansen, A. E.; Voigt, B.; Rettrup, S. Large-scale RPA calculations of chiroptical properties of organic molecules: Program RPAC. *Int. J Quant. Chem.* **1983**, *23*, 595–611.
- [17] Bouman, T. D.; Hansen, A. E. Linear response calculations of molecular optical and magnetic properties using program RPAC: NMR shielding tensors of pyridine and n-azines. *Int. J Quant. Chem.* **1989**, *36*, 381–396.
- [18] Casida, M. E. Time-Dependent Density Functional Response Theory for Molecules. Recent Advances in Density Functional Methods. pp 155–192.
- [19] Dreuw, A.; Head-Gordon, M. Single-Reference ab Initio Methods for the Calculation of Excited States of Large Molecules. *Chem. Rev.* **2005**, *105*, 4009.
- [20] de Silva, P. Inverted Singlet–Triplet Gaps and Their Relevance to Thermally Activated Delayed Fluorescence. *J. Phys. Chem. Lett.* **2019**, *10*, 5674.
- [21] Ghosh, S.; Bhattacharyya, K. Origin of the Failure of Density Functional Theories in Predicting Inverted Singlet–Triplet Gaps. *J. Phys. Chem. A* **2022**, *126*, 1378–1385.
- [22] Ricci, G.; San-Fabián, E.; Olivier, Y.; Sancho-García, J. C. Singlet-Triplet Excited-State Inversion in Heptazine and Related Molecules: Assessment of TD-DFT and ab initio Methods. *Chem. Phys. Chem.* **2021**, *22*, 553.
- [23] Li, J.; Li, Z.; Liu, H.; Gong, H.; Zhang, J.; Yao, Y.; Guo, Q. Organic molecules with inverted singlet-triplet gaps. *Front. Chem.* **2022**, *10*.
- [24] Pollice, R.; Friederich, P.; Lavigne, C.; Gomes, G. d. P.; Aspuru-Guzik, A. Organic Molecules

- with Inverted Gaps between First Excited Singlet and Triplet States and Appreciable Fluorescence Rates. *Matter* **2021**, *4*, 1654.
- [25] Sobolewski, A. L.; Domcke, W. Are Heptazine-Based Organic Light-Emitting Diode Chromophores Thermally Activated Delayed Fluorescence or Inverted Singlet-Triplet Systems? *J. Phys. Chem. Lett.* **2021**, *12*, 6852.
- [26] Dreuw, A.; Hoffmann, M. The inverted singlet–triplet gap: a vanishing myth? *Front. Chem.* **2023**, *11*.
- [27] Sanz-Rodrigo, J.; Ricci, G.; Olivier, Y.; Sancho-García, J. C. Negative Singlet–Triplet Excitation Energy Gap in Triangle-Shaped Molecular Emitters for Efficient Triplet Harvesting. *J. Phys. Chem. A* **2021**, *125*, 513.
- [28] Ehrmaier, J.; Rabe, E. J.; Pristash, S. R.; Corp, K. L.; Schlenker, C. W.; Sobolewski, A. L.; Domcke, W. Singlet-Triplet Inversion in Heptazine and in Polymeric Carbon Nitrides. *J. Phys. Chem. A* **2019**, *123*, 8099.
- [29] Pios, S.; Huang, X.; Sobolewski, A. L.; Domcke, W. Triangular boron carbon nitrides: An unexplored family of chromophores with unique properties for photocatalysis and ptoelectronics. *J. Phys. Chem. Chem. Phys.* **2021**, *23*, 12968.
- [30] Tučková, L.; Straka, M.; Valiev, R. R.; Sundholm, D. On the origin of the inverted singlet–triplet gap of the 5th generation light-emitting molecules. *J. Phys. Chem. Chem. Phys.* **2022**, *24*, 18713–18721.
- [31] Loos, P. F.; Lipparini, F.; Jacquemin, D. Heptazine, Cyclazine, and Related Compounds: Chemically-Accurate Estimates of the Inverted Singlet–Triplet Gap. *The Journal of Physical Chemistry Letters* **2023**, *14*, 11069–11075.
- [32] Runge, E.; Gross, E. K. U. Density-Functional Theory for Time Dependent Systems. *Phys. Rev. Lett.* **1984**, *52*, 997.
- [33] Rhee, Y. M.; Head-Gordon, M. Scaled Second-Order Perturbation Corrections to Configuration Interaction Singles: Efficient and Reliable Excitation Energy Methods. *J. Phys. Chem. A* **2007**, *111*, 5314.
- [34] Head-Gordon, M.; Rico, R. J.; Oumi, M.; Lee, T. J. A doubles correction to electronic excited states from configuration interaction in the space of single substitutions. *Chem. Phys. Lett.* **1994**, *219*, 21.
- [35] Stanton, J. F.; Bartlett, R. J. The equation of motion coupled-cluster method. A systematic

- biorthogonal approach to molecular excitation energies, transition probabilities, and excited state properties. *J. Chem. Phys.* **1993**, *98*, 7029.
- [36] Sancho-García, J. C.; Brémond, E.; Ricci, G.; Pérez-Jiménez, A. J.; Olivier, Y.; Adamo, C. Violation of Hund’s rule in molecules: Predicting the excited-state energy inversion by TD-DFT with double-hybrid methods. *J. Chem. Phys.* **2022**, *156*, 034105.
- [37] Hellweg, A.; Grün, S. A.; Hättig, C. Benchmarking the performance of spin-component scaled CC2 in ground and electronically excited states. *Phys. Chem. Chem. Phys.* **2008**, *10*, 4119.
- [38] Wormit, M.; Rehn, D. R.; Harbach, P. H. P.; Wenzel, J.; Krauter, C. M.; Epifanovsky, E.; Dreuw, A. Investigating excited electronic states using the algebraic diagrammatic construction (ADC) approach of the polarisation propagator. *Mol. Phys.* **2014**, *112*, 774.
- [39] Olsen, J.; Roos, B. O.; Jørgensen, P.; Jensen, H. J. A. Determinant Based Configuration Interaction Algorithms for Complete and Restricted Configuration Interaction Spaces. *J. Chem. Phys.* **1988**, *89*, 2185.
- [40] Angeli, C.; Cimiraglia, R.; Evangelisti, S.; Leininger, T.; Malrieu, J.-P. Introduction of N-electron valence states for multireference perturbation theory. *J. Chem. Phys.* **2001**, *114*, 10252.
- [41] Christiansen, O.; Koch, H.; Jørgensen, P. Response functions in the CC3 iterative triple excitation model. *The Journal of Chemical Physics* **1995**, *103*, 7429–7441.
- [42] Nooijen, M.; Bartlett, R. J. Similarity transformed equation-of-motion coupled-cluster theory: Details, examples, and comparisons. *J. Chem. Phys.* **1997**, *107*, 6812.
- [43] Ghosh, S.; Verma, P.; Cramer, C. J.; Gagliardi, L.; Truhlar, D. G. Combining Wave Function Methods with Density Functional Theory for Excited States. *Chem. Rev.* **2018**, *118*, 7249.
- [44] Grimme, S.; Neese, F. Double-Hybrid Density Functional Theory for Excited Electronic States of Molecules. *J. Chem. Phys.* **2007**, *127*, 154116.
- [45] Haase, P. A. B.; Faber, R.; Provasi, P. F.; Sauer, S. P. A. Noniterative Doubles Corrections to the Random Phase and Higher Random Phase Approximations: Singlet and Triplet Excitation Energies. *J. Comput. Chem.* **2020**, *41*, 43–55.
- [46] Szabo, A.; Ostlund, N. S. *Modern Quantum Chemistry*; Dover: New York, 1996.
- [47] Helgaker, T.; Jørgensen, P.; Olsen, J. *Molecular Electronic Structure Theory*; John Wiley and Sons, Ltd: New York, 2000.
- [48] Runge, E.; Gross, E. K. U. Density-Functional Theory for Time-Dependent Systems. *Phys.*

- Rev. Lett.* **1984**, *52*, 997–1000.
- [49] Burke, K.; Werschnik, J.; Gross, E. K. U. Time-dependent density functional theory: Past, present, and future. *The Journal of Chemical Physics* **2005**, *123*, 062206.
- [50] Gross, E. K. U.; Kohn, W. Local density-functional theory of frequency-dependent linear response. *Phys. Rev. Lett.* **1985**, *55*, 2850–2852.
- [51] Burke, K. Perspective on density functional theory. *The Journal of Chemical Physics* **2012**, *136*, 150901.
- [52] Dobson, J. F.; Wang, J. Energy-optimized local exchange-correlation kernel for the electron gas: Application to van der Waals forces. *Phys. Rev. B* **2000**, *62*, 10038–10045.
- [53] Elliott, P.; Goldson, S.; Canahui, C.; Maitra, N. T. Perspectives on double-excitations in TDDFT. *Chem. Phys.* **2011**, *391*, 110.
- [54] Gilbert, A. T. B.; Besley, N. A.; Gill, P. M. W. Self-Consistent Field Calculations of Excited States Using the Maximum Overlap Method (MOM). *J Phys. Chem. A* **2008**, *112*, 13164–13171.
- [55] Hait, D.; Head-Gordon, M. Excited State Orbital Optimization via Minimizing the Square of the Gradient: General Approach and Application to Singly and Doubly Excited States via Density Functional Theory. *J Chem. Theor. Comput.* **2020**, *16*, 1699–1710.
- [56] Hait, D.; Head-Gordon, M. Orbital optimized density functional theory for electronic excited states. *J. Phys. Chem. Lett.* **2021**, *12*, 4517.
- [57] Hait, D.; Zhu, T.; McMahon, D. P.; Van Voorhis, T. Prediction of Excited-State Energies and Singlet–Triplet Gaps of Charge-Transfer States Using a Restricted Open-Shell Kohn–Sham Approach. *J Chem. Theor. Comput.* **2016**, *12*, 3353–3359.
- [58] Cheng, C.-L.; Wu, Q.; Van Voorhis, T. Rydberg energies using excited state density functional theory. *The Journal of Chemical Physics* **2008**, *129*, 124112.
- [59] Lischka, H.; Nachtigallová, D.; Aquino, A. J. A.; Szalay, P. G.; Plasser, F.; Machado, F. B. C.; Barbatti, M. Multireference Approaches for Excited States of Molecules. *Chem. Rev.* **2018**, *118*, 7293–7361.
- [60] Andersson, K.; Malmqvist, P. A.; Roos, B. O.; Sadlej, A. J.; Wolinski, K. Second-order perturbation theory with a CASSCF reference function. *J. Phys. Chem.* **1990**, *94*, 5483–5488.
- [61] Andersson, K.; Malmqvist, P.; Roos, B. O. Second-order perturbation theory with a complete active space self-consistent field reference function. *J. Chem. Phys.* **1992**, *96*, 1218–1226.

- [62] Hirao, K. Multireference Møller-Plesset method. *Chem. Phys. Lett.* **1992**, *190*, 374–380.
- [63] Kozłowski, P. M.; Davidson, E. R. Considerations in constructing a multireference second-order perturbation theory. *J. Chem. Phys.* **1994**, *100*, 3672–3682.
- [64] Hoffmann, M. R. Canonical Van Vleck Quasidegenerate Perturbation Theory with Trigonometric Variables. *J. Phys. Chem.* **1996**, *100*, 6125–6130.
- [65] Sen, A.; Sen, S.; Samanta, P. K.; Mukherjee, D. Unitary group adapted state specific multireference perturbation theory: Formulation and pilot applications. *J. Comput. Chem.* **2015**, *36*, 670–688.
- [66] Werner, H.-J.; Knowles, P. J. An efficient internally contracted multiconfiguration-reference configuration interaction method. *J. Chem. Phys.* **1988**, *89*, 5803.
- [67] Jeziorski, B.; Monkhorst, H. J. Coupled-cluster method for multideterminantal reference states. *Phys. Rev. A* **1981**, *24*, 1668–1681.
- [68] Li, X.; Paldus, J. Unitary group based state-selective coupled-cluster method: Comparison of the first order interacting space and the full single and double excitation space approximations. *J. Chem. Phys.* **1995**, *102*, 8897–8905.
- [69] Li, X.; Paldus, J. Reduced multireference CCSD method: An effective approach to quasidegenerate states. *J. Chem. Phys.* **1997**, *107*, 6257–6269.
- [70] Mahapatra, U. S.; Datta, B.; Mukherjee, D. A state-specific multi-reference coupled cluster formalism with molecular applications. *Mol. Phys.* **1998**, *94*, 157–171.
- [71] Mahapatra, U. S.; Datta, B.; Bandyopadhyay, B.; Mukherjee, D. In *State-Specific Multi-Reference Coupled Cluster Formulations: Two Paradigms*; Löwdin, P.-O., Ed.; Advances in Quantum Chemistry; Academic Press, 1998; Vol. 30; pp 163–193.
- [72] Aoto, Y. A.; Köhn, A. Internally contracted multireference coupled-cluster theory in a multi-state framework. *J. Chem. Phys.* **2016**, *144*, 074103.
- [73] Szalay, P. G.; Bartlett, R. J. Approximately extensive modifications of the multireference configuration interaction method: A theoretical and practical analysis. *J. Chem. Phys.* **1995**, *103*, 3600–3612.
- [74] Neese, F.; Wennmohs, F.; Becker, U.; Riplinger, C. The ORCA quantum chemistry program package. *J. Chem. Phys.* **2020**, *152*, 224108.
- [75] Shao, Y.; Gan, Z.; Epifanovsky, E.; Gilbert, A. T.; Wormit, M.; Kussmann, J.; Lange, A. W.; Behn, A.; Deng, J.; Feng, X. Advances in molecular quantum chemistry contained in the

- Q-Chem 4 program package. *Mol. Phys.* **2015**, *113*, 184.
- [76] Weigend, F.; Ahlrichs, R. Balanced basis sets of split valence, triple zeta valence and quadruple zeta valence quality for H to Rn: Design and assessment of accuracy. *Phys. Chem. Chem. Phys.* **2005**, *7*, 3297.
- [77] Stanton, J. F. Why CCSD(T) works: a different perspective. *Chem. Phys. Lett.* **1997**, *281*, 130–134.
- [78] Raghavachari, K.; Trucks, G. W.; Pople, J. A.; Head-Gordon, M. A fifth-order perturbation comparison of electron correlation theories. *Chem. Phys. Lett.* **1989**, *157*, 479–483.
- [79] Dunning, J., Thom H. Gaussian basis sets for use in correlated molecular calculations. I. The atoms boron through neon and hydrogen. *J. Chem. Phys.* **1989**, *90*, 1007–1023.
- [80] Becke, A. D. Density-functional thermochemistry. III. The role of exact exchange. *J. Chem. Phys.* **1993**, *98*, 5648.
- [81] Grimme, S.; Ehrlich, S.; Goerigk, L. Effect of the damping function in dispersion corrected density functional theory. *J. Comput. Chem.* **2011**, *32*, 1456–1465.
- [82] Bhattacharyya, K. Can TDDFT Render the Electronic Excited States Ordering of Azine Derivative? A Closer Investigation with DLPNO-STEOM-CCSD. *Chem. Phys. Lett.* **2021**, *779*, 138827.
- [83] Stanton, J. F. On the extent of spin contamination in open-shell coupled-cluster wave functions. *J Chem. Phys.* **1994**, *101*, 371–374.
- [84] Drwal, D.; Matousek, M.; Golub, P.; Tucholska, A.; Hapka, M.; Brabec, J.; Veis, L.; Pernal, K. Role of Spin Polarization and Dynamic Correlation in Singlet–Triplet Gap Inversion of Heptazine Derivatives. *J Chem. Theor. Comput.* **2023**, *19*, 7606–7616.
- [85] Ye, H. Z.; Voorhis, T. V. Self-consistent Møller-Plesset Perturbation Theory For Excited States. *arXiv preprint arXiv: 2008.10777* **2020**,
- [86] Rettig, A.; Hait, D.; Bertels, L. W.; Head-Gordon, M. Third-Order Møller–Plesset Theory Made More Useful? The Role of Density Functional Theory Orbitals. *Journal of Chemical Theory and Computation* **2020**, *16*, 7473–7489.
- [87] Fang, Z.; Lee, Z.; Peterson, K. A.; Dixon, D. A. Use of Improved Orbitals for CCSD(T) Calculations for Predicting Heats of Formation of Group IV and Group VI Metal Oxide Monomers and Dimers and UCl₆. *Journal of Chemical Theory and Computation* **2016**, *12*, 3583–3592.

- [88] Beran, G. J. O.; Gwaltney, S. R.; Head-Gordon, M. Approaching closed-shell accuracy for radicals using coupled cluster theory with perturbative triple substitutions. *Phys. Chem. Chem. Phys.* **2003**, *5*, 2488–2493.
- [89] Mallick, S.; Rai, P. K.; Kumar, P. Accurate estimation of singlet-triplet gap of strongly correlated systems by CCSD(T) method using improved orbitals. *Comput. Theor. Chem.* **2021**, *1202*, 113326.
- [90] Alipour, M.; Izadkhast, T. Do any types of double-hybrid models render the correct order of excited state energies in inverted singlet–triplet emitters? *J Chem. Phys.* **2022**, *156*, 064302.
- [91] New diagnostics for coupled-cluster and Møller–Plesset perturbation theory. *Chemical Physics Letters* **1998**, *290*, 423–430.
- [92] Lee, T. J.; Taylor, P. R. A diagnostic for determining the quality of single-reference electron correlation methods. *International Journal of Quantum Chemistry* **1989**, *36*, 199–207.
- [93] Bao, J. J.; Truhlar, D. G. Automatic Active Space Selection for Calculating Electronic Excitation Energies Based on High-Spin Unrestricted Hartree–Fock Orbitals. *J Chem. Theor. Comput.* **2019**, *15*, 5308–5318.
- [94] Golub, P.; Antalík, A.; Veis, L.; Brabec, J. Machine Learning-Assisted Selection of Active Spaces for Strongly Correlated Transition Metal Systems. *J Chem. Theor. Comput.* **2021**, *17*, 6053–6072.
- [95] Stein, C. J.; Reiher, M. autoCAS: A Program for Fully Automated Multiconfigurational Calculations. *J. Comput. Chem.* **2019**, *40*, 2216–2226.
- [96] King, D. S.; Gagliardi, L. A Ranked-Orbital Approach to Select Active Spaces for High-Throughput Multireference Computation. *J Chem. Theor. Comput.* **2021**, *17*, 2817–2831.
- [97] Veryazov, V.; Malmqvist, P. A.; Roos, B. O. How to select active space for multiconfigurational quantum chemistry? *Int. J Quant. Chem.* **2011**, *111*, 3329–3338.
- [98] Loos, P. F.; Boggio Pasqua, M.; Scemama, A.; Caffarel, M.; Jacquemin, D. Reference energies for double excitations. *J. Chem. Theory Comput.* **2019**, *15*, 1939.

